Macromolecules
ARTICLE

Macromolecules **2010**, *43*, 3935–3940 **3935**
DOI: 10.1021/ma100176f

Evaluation of Gelation Kinetics of Tetra-PEG Gel

Manami Kurakazu,[†,∥] Takuya Katashima,[†,∥] Masashi Chijiishi,[†] Kengo Nishi,[†] Yuki Akagi,[†] Takuro Matsunaga,[§] Mitsuhiro Shibayama,[§] Ung-il Chung,[†] and Takamasa Sakai*[,†]

[†]*Department of Bioengineering, Graduate School of Engineering, The University of Tokyo, 7-3-1 Hongo, Bunkyo-ku, Tokyo 113-8656, Japan, and* [§]*The Institute for Solid State Physics, The University of Tokyo, 5-1-5 Kashiwanoha, Kashiwa, 277-8581, Japan.* [∥] *These authors contributed equally to the work.*

Received January 23, 2010

ABSTRACT: Polymer gels formed from A-B type of coupling reaction were investigated vigorously as a "model network" because the mesh size of the network was defined by the size and shape of the building blocks. However, the formation of these networks has an inherent difficulty in homogeneous mixing of mutually reactive building blocks, leading to the formation of inhomogeneous network structures. Recently, we have designed and fabricated the Tetra-PEG gel by combining two well-defined symmetrical tetra-arm polymers of the same size. Although this gel was formed by simply mixing two polymer solutions, the structure was extremely homogeneous. In this study, we investigated the gelation kinetics of Tetra-PEG gel in detail. The reaction kinetics corresponded well with the theoretical prediction, suggesting the homogeneous reacting system. This homogeneous reacting system may contribute to the homogeneous network structure of Tetra-PEG gel.

Introduction

Hydrogels are expected to have high biocompatibility because of their high water content of up to 90%. Because they offer the 3D space capable of containing the drugs and cells, hydrogels are applied in biomedical fields.[1−3] In particular, on-site-forming hydrogels are useful in biomedical applications such as artificial scaffolds for tissue regeneration and drug reservoirs for drug delivery systems,[4,5] because they can be injected into the body in a minimally invasive way. The fabrication methods for on-site forming gels are classified roughly into two categories: the reaction initiated by external stimuli[6,7] and A-B type polycondensation between mutually reactive building blocks.[8,9]

The second type of gels formed from building blocks has been investigated vigorously as a "model network" because the mesh size of the network was controllable through the precise polymerization of the building blocks.[10,11] The controllability is also favorable in biomedical applications because the characteristics of polymer gels including the elastic modulus and diffusion property of the contained drug are predictable. Furthermore, a homogeneous network is expected to have high mechanical strength, which is one of the most desired properties of polymer gels. However, model networks invented so far had the same order of mechanical strength as that of the other conventional networks. Although the model networks were more homogeneous than the other conventional polymer networks, the network homogeneity was insufficient to achieve the high mechanical strength. The substantial amount of spatial and the topological inhomogeneities was detected in model networks.[10,12,13] Although there are several possible causes introducing the inhomogeneities, the inhomogeneous mixing of building blocks seems to be an inherent problem in the A-B type polycondensation reaction.[14] Because the inhomogeneous mixing introduces the microscopic stoichiometric imbalance, it reduces not only the reaction rate but also the reaction conversion.[15] Especially in the gelling system because the viscosity increases dramatically at the gelation threshold, and the unreacted building blocks cannot diffuse macroscopically to find the reactive groups.[16−18] Although the polymeric reaction kinetics[19−21] and gelation threshold[15,22−24] were discussed by many researchers, the evaluation of gelation kinetics, especially in the viewpoint of chemical reaction theory, has not been achieved as far as we know.

Recently, as a new class of model networks, we have designed and fabricated the Tetra-PEG gel by combining two mutually reactive tetra-arm polymers of the same size.[25] Although this gel is formed by mixing two polymer solutions within a few minutes, the inhomogeneities are strongly suppressed. The spatial inhomogeneities were extremely low in the detectable range of the SANS measurement, that is, 0.003 $Å^{-1}$ (∼2000 Å).[26,27] The topological inhomogeneities such as entanglements and loops are much fewer than conventional model networks.[28] In addition, the breaking strength was superior to the conventional model networks and was comparable to that of the native articular cartilage (6−10 MPa).[29] These results suggest that the Tetra-PEG gel has extremely homogeneous network structure.

The reacting system of Tetra-PEG gel is likely to be different from the conventional model networks. Our previous SANS result suggests that the tetra-arm polymer, which is the building block of the Tetra-PEG gel, behaves as an impenetrable space-filling sphere in the semidilute solution. This situation is different from that of the linear polymers, which easily penetrate each other in the semidilute solution. This non-entangling nature of tetra-arm polymers is expected to contribute to the homogeneous mixing of two building blocks, that is, homogeneous reaction system. When the gelation is proceeding in the homogeneous system, we can describe the gelation kinetics simply by considering the reaction between the mutually reactive end groups. In this study, we tried to describe the gelation kinetics of Tetra-PEG gel by considering the simple A-B-type reaction of mutually reactive end groups.

Figure 1 shows the elementary step of this gelation reaction, which is a reaction between the amine group and the activated

*To whom correspondence should be addressed. Tel: +81-3-5841-1899. Fax: +81-3-5841-8843. E-mail: sakai@tetrapod.t.u-tokyo.ac.jp.

Published on Web 03/10/2010

ester group forming the amide bond. Here three points should be noted. First, only the un-ionized amine group has the reactivity with the activated ester group because the ionized amine group does not have an unshared electron pair. Second, the ionized amine groups are expected to diffuse faster than the other un-ionized units because the fluctuating local electric field drives the polymer diffusion.[30,31] This electrostatic effect is expected to contribute to the homogeneous mixing. Third, the activated ester group will be hydrolyzed over time. We investigated these three effects on the gelation process and postgelation properties by measuring the gelation time (t_{gel}), reaction rate constant (k_{gel}), the elastic modulus (G'), and reaction efficiency (p). We investigated the effect of the ratio of ionized to un-ionized amine groups by changing the pH. The electrostatic effect of amine groups on the diffusion was investigated by changing the ionic strength. The hydrolysis of the activated ester group was investigated by UV spectroscopy.

Experimental Section

Materials. Tetra-amine-terminated PEG (TAPEG) and tetra-NHS-glutarate-terminated PEG (TNPEG) were prepared from tetra-hydroxyl-terminated PEG (THPEG) having equal arm lengths. The details of TAPEG and TNPEG preparation were previously reported.[25] The molecular weights (M_w) of TAPEG and TNPEG were matched to be 10 kg/mol. Here NHS represents *N*-hydroxysuccinimide. The activity of the functional groups was estimated using NMR. TNPEG ^{1}H NMR ($CDCl_3$, δ): 2.07 (m, 2H, CH_2 CH_2 CH_2), 2.49 (t, 2H, CH_2 CH_2 CH_2), 2.72 (t, 2H, CH_2 CH_2 CH_2), 2.83 (s, 4H, NCO CH_2 CH_2CON), 3.4 (s, 2H, CH_2O), 3.63(m, (4 m − 2)H, (CH_2 CH_2O)$_{m-1}$ CH_2), 4.24 (t, 2H, CH_2CH_2O). TAPEG ^{1}H NMR ($CDCl_3$, δ): 1.91 (br, 2H, NH_2), 3.18 (t, 2H, CH_2 CH_2), 3.42 (s, 2H, CH_2O), 3.63 (m, (4 m − 2)H, (CH_2 CH_2O)$_{m-1}$$CH_2$).

Potentiometric Titration. TAPEG (125 mg) was dissolved in 50 mL of 0.001 N HCl. The resultant solution was titrated at 25 °C with 0.01 N NaOH. The NaOH solution was added in quantities of 5 μL after the pH values were stabilized (minimal interval: 30 s) using an automatic titrator (TS-2000, Hiranuma, Japan).

Degradation of NHS-Glutarate. A constant amount of TNPEG (15−30 mg) was dissolved in 3.0 mL of 0.2 M phosphate buffer (pH 5.8, 7.0, 8.0). The time course of absorbance at 290 nm was measured by UV spectromether (JASCO V-670DS, Nihon-bunko, Japan). The standard curve was obtained by measuring the absorbance at 290 nm of *N*-hydroxylsuccinimide buffer solutions (0.016 to 1.0 mM).

pH Measurement of Pregel Solutions. A constant amount of TAPEG (225 mg) was dissolved into 7.5 mL of phosphate buffer solution (PB; 31.2 mM, pH7.4) or citric-phosphate buffer solution (CPB; 31.2 mM, pH5.8) or mixed solutions (Table 1). Then, the pH was measured with a pH meter (SevenMulti580, Mettler Toledo, Switzerland) at 20 °C.

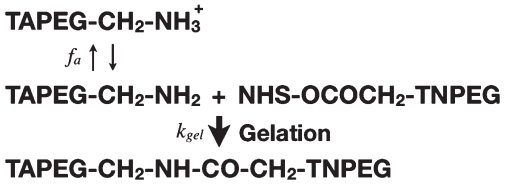

Figure 1. Schematic model of the elementary steps for this gelation reaction. f_a and k_{gel} are the fraction of un-ionized amine group and the reaction rate constant, respectively.

Measurement of Sol Fraction. The gel was fabricated into rectangular films (30 mm high, 5 mm wide, 2 mm thick). The obtained gels (~3 g) were immersed in 150 mL of H_2O at 37 °C for 48 h with shaking. The extracted solution was concentrated to ~10 mL and then freeze-dried. The element composition of the soluble component was measured using a thermogravimetry analyzer (TG/DTA 6200) from 30 to 500 °C at a heating rate of 10 °C/min under nitrogen flow (20 mL/min). The sol fraction was obtained using the total amount of sol fraction and the element composition of PEG.[28]

pH and Ionic Strength Dependence of Gelation Process and Postgelation Properties. To control the pH, constant amounts of TAPEG and TNPEG (450 mg) were dissolved in 7.5 mL of phosphate buffer solution (PB; 31.2 mM, pH 7.4) or citric-phosphate buffer solution (CPB; 31.2 mM, pH5.8) or mixed solutions (Table 1). It is known that the NHS-glutarate dissociates in the buffer solution and the hydrolysis is faster at higher pH.[32] Therefore, we used the citric-phosphate buffer solution (pH 5.8) for TNPEG to a maximum extent. To control the ionic strength, constant amounts of TAPEG and TNPEG (450 mg) were dissolved in 7.5 mL of phosphate buffer solutions (PB; 31.2 mM, pH 7.4) and citric-phosphate buffer solutions (CPB; 31.2 mM, pH 5.8) including 50, 100, and 150 mM of KCl, respectively. The two solutions were mixed in a 50 mL Falcon tube for 10 s using the voltex mixer (Delta mixer Se-08, Taitec, Japan). Then, the resultant solution was poured in the interstice of the double cylinder of a rheometer (MCR501, Anton Paar, Austria). The oscillatory shear rheological properties, that is, the storage elastic modulus (G') and the loss elastic modulus (G''), during gelation were measured at 20 °C with a double cylinder geometry with 26.7 and 28.9 mm diameter cylinders. The sampling time interval was changed from 20 to 100 s without intermission for 8 h. The strain and the frequency were 2% and 1 Hz, respectively. Rheological properties after the gelation were measured at 8 h after mixing at a constant strain (1%) and a constant frequency (1 Hz) at 20 °C.

Results and Discussion

Ionization Degree of TAPEG. Figure 2 shows the ionization degree of TAPEG as a function of pH. The pK_a of the amine group of TAPEG was estimated to be 9.27. It was revealed that almost all amine groups are ionized and therefore cannot react with the activated ester group when we set the reaction condition near the biological pH. Therefore, the rate-limiting factor of this gelation reaction is expected to be the ratio of un-ionized amine groups to the whole amine groups. Here it should be noted that the pH of the pregel solutions was higher than the value defined by the corresponding buffer solutions because of the ionization of amine groups (Table 1).

Hydrolysis of TNPEG. We measured the degradation of NHS-glutarate at several pH points. Because only the ionized NHS have the absorbance at 290 nm,[33] it was necessary

Table 1. Buffers Used and Initial pH of Gelling Solution

		solvent of TAPEG		solvent of TNPEG	
sample no.	initial pH of gelling solution	PB (mL)	CPB (mL)	PB (mL)	CPB (mL)
1	7.0	0	7.500	0	7.500
2	7.4	3.750	3.750	0	7.500
3	7.6	5.625	1.875	0	7.500
4	8.0	7.500	0	0	7.500
5	8.2	7.500	0	3.750	3.750
6	8.7	7.500	0	5.0	2.500
7	9.2	7.5	0	7.5	0

to obtain the standard curve under each pH condition. Figure 3 shows the fraction of the nondegraded activated ester groups (f_n, solid curve) as a function of time. The f_n is represented as

$$f_n = \exp(-k_{deg}t) \quad (1)$$

Here k_{deg} and t are the degradation rate constant and time, respectively. As shown in Figure 3, the experimental result deviated upward from the theoretical correlation, that is, $-\ln(f_n) \sim t$, with time. It is because the degraded NHS group acts as an acid that decreases the pH of the solution. Therefore, the experimental data within 500 s were used for fitting with eq 1 (dotted lines). The half-life of the activated ester (τ_{NHS}) at pH 5.8, 7.0, and 8.0 was estimated to be 12 600, 7830, 5230 s, respectively. These values corresponded well with the value previously reported by Nojima et al.[32] In the following experiment, we measured the gelation process for 8 h because almost all of the activated ester was expected to be degraded by 8 h, even at pH 7.

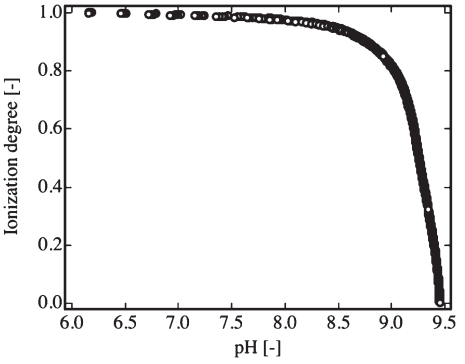

Figure 2. Ionization degree of TAPEG as a function of pH. The α-pH curve was determined from the titration curves obtained at 25 °C.

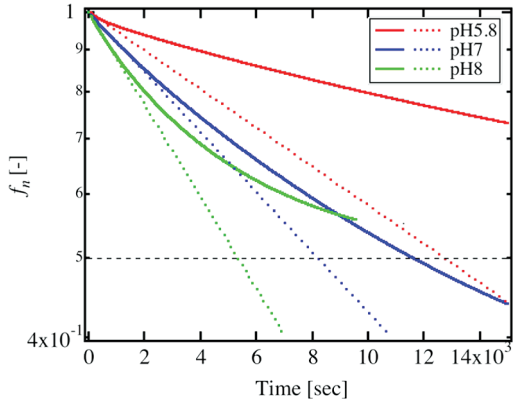

Figure 3. Degradation rates of NHS-glutarate in buffer solutions (pH 5.8 (red), 7.0 (blue), and 8.0 (green)). The solid and dotted lines represent the experimental results and fitting results, respectively.

pH Dependence of Gelation Process and Postgelation Properties. The evolution of the oscillatory shear moduli was used to monitor the viscoelastic properties during the gelation process. The gelation point (t_{gel}) in rheological curves was defined according to the criteria of Chambon and Winter (i.e., G', $G'' \sim \omega^n$, or $\tan\delta$ = unity) or simply as the crossover of the storage modulus G' and the loss modulus G''.[34,35] The initial pH of the gelling solutions was changed from 7.0 to 9.2 (Table 1), corresponding to the change in the un-ionized amine fraction (f_a) from 0.008 to 0.3 (Figure 2). Although the initial pH of the gelling solution was higher than that of the corresponding buffer solution, the pH decreased to the value defined by the buffer solution as the reaction proceeded. Because the amount of activated ester is much larger than that of reactive un-ionized amine, this reaction is reduced to a pseudo-first-order reaction of un-ionized amine.[36] Therefore, the reaction rate is given by

$$\frac{dx}{dt} = k_{gel}[NH_2] = k_{gel}f_a(a-x) \quad (2)$$

Here k_{gel}, f_a, a, and x denote the reaction rate constant, the fraction of un-ionized amine groups, the initial concentration of amine and activated ester, and the concentration of the amide bond, respectively. Here we use constant f_a at the initial solution. From eq 2, x is represented as follows

$$x = a(1-\exp(-k_{gel}f_a t)) \quad (3)$$

Because the gelation threshold is calculated as $x = a/3$ for the gelation from tetrafunctional polymers,[23] the gelation time (t_{gel}) is estimated to be

$$t_{gel} = \ln\left(\frac{3}{2}\cdot\frac{1}{k_{gel}f_a}\right) \quad (4)$$

According to eq 4, t_{gel} is expected to be inversely proportional to the f_a.

Figure 4A shows t_{gel} determined by rheometry as a function of f_a. The fitting result in the region $0.013 < f_a < 0.08$ shows the relationship as, $t_{gel} \sim f_a^{-1.09}$, suggesting the consistency of eq 4. We calculated the k_{gel} using the eq 4 and then plotted against the f_a (Figure 4B). The value of k_{gel} was almost constant in the range where the t_{gel} was inversely proportional to the f_a, suggesting the homogeneous mixing.[15]

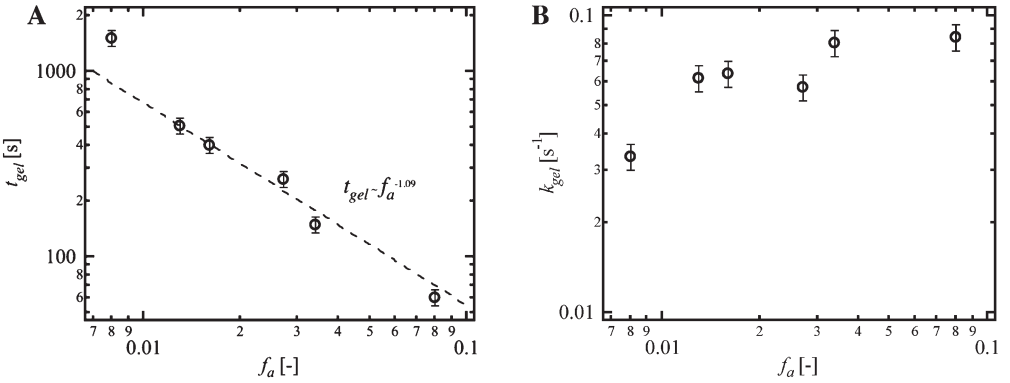

Figure 4. (A) Gelation time (t_{gel}) determined by the crossover of G' and G'' as a function of f_a. The dashed line is the fitted line of eq 4 in the range $0.013 < f_a < 0.08$. (B) k_{gel} against the initial fraction of f_a.

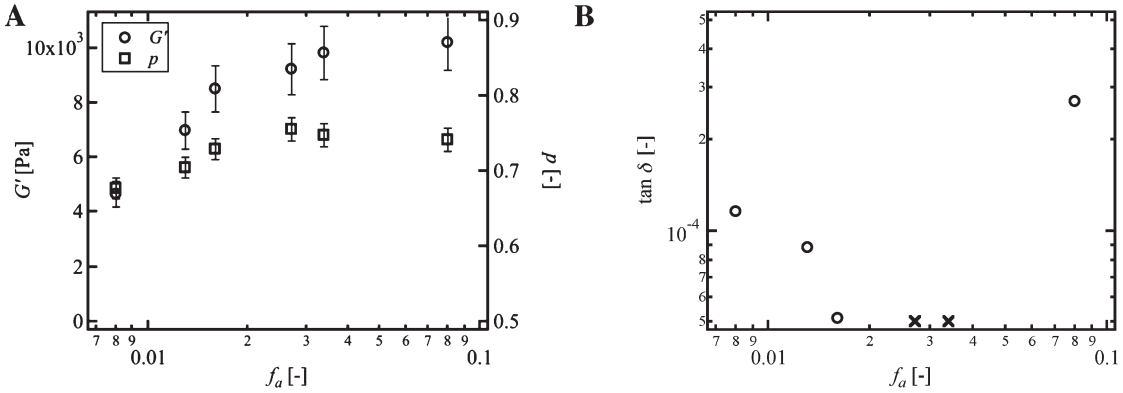

Figure 5. (A) Equilibrium value of storage modulus (G') and reaction efficiency (p) against the initial fraction of f_a. (B) Equilibrium value of tan δ as a function of f_a.

At $f_a = 0.008$, the k_{gel} was lower than the value obtained in the region $0.013 < f_a < 0.08$. It is due to the dissociation of the activated ester groups; that is, the reaction rate was too slow, and the gelation time was comparable to the τ_{NHS}. In contrast, when the f_a was 0.3, the pregel solution gelled partially, and the determination of t_{gel} was impossible because the t_{gel} was too fast (data not shown). This result strongly suggests that polymers react with each other before they are mixed homogeneously in the higher f_a region.

To investigate the effect of f_a on postgelation properties, we plotted the equilibrium value of G' and p as a function of f_a (Figure 5). The G' and p increased asymptotically as f_a increased; in the region $0.03 < f_a$, G' and p became constant. This tendency is explained as follows. Although the t_{gel} is smaller than τ_{NHS}, the total reaction time (8 h) is larger than τ_{NHS}. The gelation reaction competes with degradation of NHS-glutarate. Therefore, the p increased as reaction rate increased. The constant reaction conversion in the region $0.03 < f_a$ is probably due to the topological restriction of reactive end groups connected to the polymer network structure.[28] Similar tendency was reported in the gelation system using the vinylsulfonate and the thiol as a reactive species.[37] Figure 5B shows the tan δ, which is the indicator of mechanical dissipation as a function of f_a. Around the $f_a = 0.03$, tan δ was too small to be detected by a rheometer; the minimum measurement limit of tan δ was $\approx 5 \times 10^{-5}$. These data suggest that the most homogeneous network structure was formed in this region. This region corresponds to the region where the plateau of G' and p appeared. This result is interpreted as follows. In the lower f_a region, the substantial number of dangling chains is formed because the dissociation of the activated ester groups decreases the reaction conversion. In the higher f_a region, the inhomogeneous distribution of polymer segment is formed in the polymer network because the polymers react with each other before they are mixed homogeneously.

The schematic image under high pH condition is depicted in Figure 6. Under high pH condition, the reaction occurs before the polymers are mixed homogeneously, and premature clusters are formed because too many NH_2 species are activated. Because few NH_2 species are activated under low pH condition, the reaction rate is slow, and activated ester groups dissociate before reacting with amine groups. In the medium pH region, the k_{gel} became constant, suggesting that the gelation kinetics is well described by the scheme shown in Figure 1. As a result, the most homogeneous network structure was formed at around $f_a = 0.03$ because the reaction rate was much faster than the degradation rate and was slow enough to allow the homogeneous mixing.

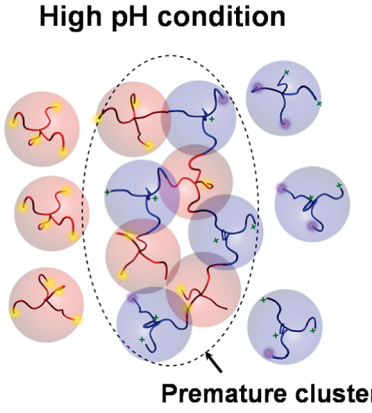

Figure 6. Schematic model of the mixing state of macromers under high pH condition.

Ionic Strength Dependence of Gelation Process and Postgelation Properties. Because the inhomogeneous gel was formed under higher pH condition, it is expected that the diffusion of the building blocks affect the reaction rate constant. The diffusion of ionized polymers in the presence of additional salt are represented as[38]

$$D = \frac{T}{\eta_0} \cdot \frac{Z_p{}^2\sqrt{C}}{Z_c{}^2C + 2I} \tag{5}$$

Here T is absolute temperature, η_0 is the viscosity of solvent, Z_p is the fraction of ionic unit in polymer, Z_c is the valence of counterion, and c is the concentration of polyelectrolyte. In the diffusion-controlled polymeric reaction, because the reaction rate constant (k_d) is proportional to the diffusion coefficient of the polymer,[19,39] k_d is represented as

$$k_d \sim D \sim \frac{\sqrt{C}}{Z_c{}^2C + 2I} \tag{6}$$

As shown in Figure 7A, the t_{gel} increased as I increased, suggesting the contribution of ionic strength on the reaction. Here it should be noted that degradation of NHS-glutarate had little effect on these results because the t_{gel} is much shorter than τ_{NHS}; the t_{gel} was in the range where the k_{gel} was constant, that is, $t_{gel} \sim f_a{}^{-1.09}$, in Figure 4. We plotted the value of k_{gel} against the value of $C^{1/2}/(Z_c{}^2C + 2I)$ (Figure 7B). A linear correlation between k_{gel} and $C^{1/2}/(Z_c{}^2C + 2I)$ was obtained, suggesting that the consistency of eq 6.

As for the postgelation properties, G' and p decreased as I increased, also suggesting the gelation reaction was inhibited

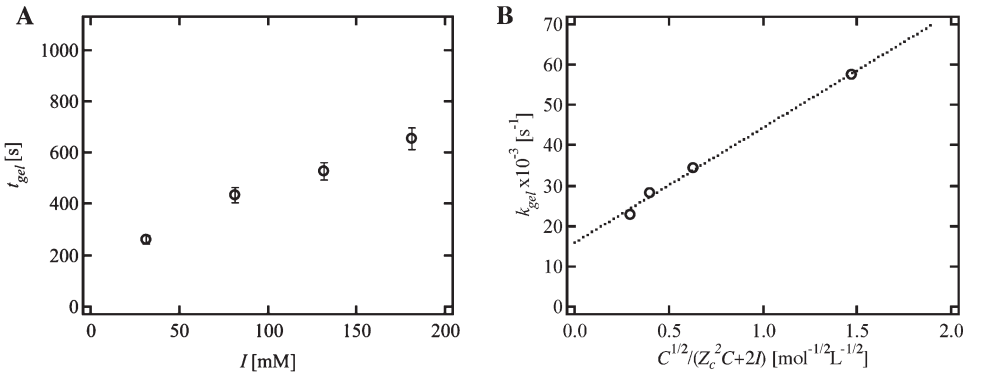

Figure 7. (A) Gelation time (t_{gel}) determined by the crossover of G' and G'' as a function of I. (B) k_{gel} as a function of $C^{1/2}/(Z_c^2C + 2I)$. The dashed line is the fitting curve of eq 6.

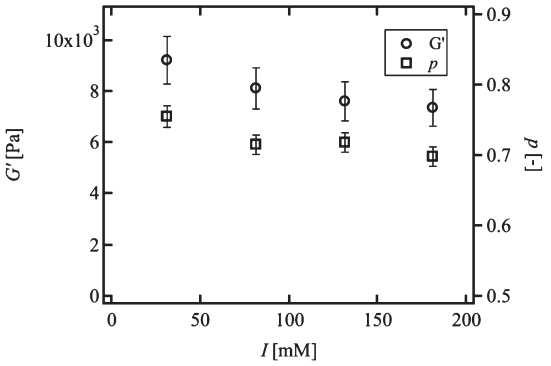

Figure 8. Equilibrium value of storage modulus (G') and reaction efficiency (p) as a function of I.

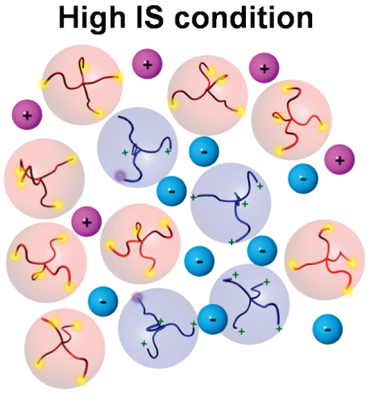

Figure 9. Schematic model of the mixing state of polymers under high I condition.

under high I condition (Figure 8). These results are also explained by the competition between the gelation reaction and the dissociation of NHS-glutarate. The tan δ obtained in this I region was too small to be detected by a rheometer (tan $\delta < 5 \times 10^{-5}$) (data not shown). Although the ionized amine groups do not have reactivity, the accelerated diffusion of the ionized amine groups contribute to the high reaction rate and reaction efficiency (Figure 9).

Conclusions

The major findings of this article are as follows: in the Tetra-PEG gel system, the gelation kinetics obeyed the theoretical prediction represented by eqs 4 and 6, suggesting the homogeneous reacting system. To obtain a homogeneous network structure, two parameters are important, that is, the pH and ionic

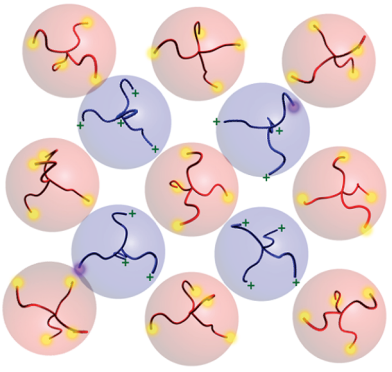

Figure 10. Schematic model of the homogeneous mixing state of polymers under optimal condition.

strength. The pH is important for controlling the reaction rate. The reaction rate must surpass the dissociation rate of activated ester and be slow enough to allow homogeneous mixing of building blocks. If the reaction rate is too fast, then the building blocks cannot be mixed homogeneously, thus forming an inhomogeneous network structure. It is noteworthy that the optimal reaction condition is near the biological pH. The ionic strength is important for controlling the diffusion coefficient of ionic amine. The ionic strength must be small enough not to inhibit the diffusion. As a result, the most homogeneous network structure was obtained at the most homogeneous reacting condition (f_a = 0.03) (Figure 10). This homogeneous reacting system may contribute to the homogeneous network structure of Tetra-PEG gel.

References and Notes

(1) Drury, J. L.; Mooney, D. J. *Biomaterials* **2003**, *24*, 4337–4351.
(2) Barcili, B. *J. Pharm. Sci.* **2007**, *96*, 2197–2223.
(3) Peppas, N. A.; Hilt, J. Z.; Khademhosseini, A.; Langer, R. *Adv. Mater.* **2006**, *18*, 1345–1360.
(4) Bryant, S. J.; Bender, R. J.; Durand, K. L.; Anseth, K. S. *Biotechnol. Bioeng.* **2004**, *86*, 747–755.
(5) Azab, A. K.; Orkin, B.; Doviner, V.; Nissan, A.; Klein, M.; Srebnik, M.; Rubinstein, A. *J. Controlled Release* **2006**, *111*, 281–289.
(6) Nguyen, K. T.; West, J. L. *Biomaterials* **2002**, *23*, 4307–4314.
(7) Weiner, A. A.; Bock, E. A.; Gipson, M. E.; Shastri, V. P. *Biomaterials* **2008**, *29*, 2400–2407.
(8) Berger, J.; Reist, M.; Mayer, J. M.; Felt, O.; Peppas, N. A.; Gurny, R. *Eur. J. Pharm. Biopharm.* **2004**, *57*, 19–34.
(9) Hiemstra, C.; Zhong, Z. Y.; Li, L. B.; Dijkstra, P. J.; Feijen, J. *Biomacromolecules* **2006**, *7*, 2790–2795.
(10) Shibayama, M.; Takahashi, H.; Nomura, S. *Macromolecules* **1995**, *28*, 6860–6864.
(11) Malkoch, M.; Vestberg, R.; Gupta, N.; Mespouille, L.; Dubois, P.; Mason, A. F.; Hedrick, J. L.; Liao, Q.; Frank, C. W.; Kingsbury, K.; Hawker, C. J. *Chem. Commun.* **2006**, *26*, 2774–2776.

(12) Villar, M. A.; Valles, E. M. *Macromolecules* **1996**, *29*, 4081–4089.
(13) Patel, S. K.; Malone, S.; Cohen, C.; Gillmor, J. R.; Colby, R. H. *Macromolecules* **1992**, *25*, 5241–5251.
(14) Hild, G. *Prog. Polym. Sci.* **1998**, *23*, 1019–1149.
(15) Flory, P. J., *Principles of Polymer Chemistry*; Cornell University Press: Ithaca, NY, 1953.
(16) Gordon, M.; Roe, R. J. *J. Polym. Sci.* **1956**, *21*, 27–37.
(17) Gordon, M.; Roe, R. J. *J. Polym. Sci.* **1956**, *21*, 39–56.
(18) Dusek, K. *Polym. Gels Networks* **1996**, *4*, 383–404.
(19) Doi, M. *Chem. Phys.* **1975**, *11*, 115–121.
(20) Degennes, P. G. *J. Chem. Phys.* **1982**, *76*, 3316–3321.
(21) Oshaughnessy, B. *Macromolecules* **1994**, *27*, 3875–3884.
(22) Stauffer, D. *J. Chem. Soc., Faraday Trans. II* **1976**, *72*, 1354–1364.
(23) Miller, D. R.; Macosko, C. W. *Macromolecules* **1976**, *9*, 206–211.
(24) Dusek, K.; Gordon, M.; Rossmurphy, S. B. *Macromolecules* **1978**, *11*, 236–245.
(25) Sakai, T.; Matsunaga, T.; Yamamoto, Y.; Ito, C.; Yoshida, R.; Suzuki, S.; Sasaki, N.; Shibayama, M.; Chung, U. I. *Macromolecules* **2008**, *41*, 5379–5384.
(26) Matsunaga, T.; Sakai, T.; Akagi, Y.; Chung, U.; Shibayama, M. *Macromolecules* **2009**, *42*, 1344–1351.
(27) Matsunaga, T.; Sakai, T.; Akagi, Y.; Chung, U. I.; Shibayama, M. *Macromolecules* **2009**, *42*, 6245–6252.
(28) Akagi, Y.; Matsunaga, T.; Shibayama, M.; Chung, U.; Sakai, T. *Macromolecules* **2010**, *43*, 488–493.
(29) Abe, H.; Hayashi, K.; Sato, M. *Data Book of Mechanical Properties of Living Cells, Tissues, and Organs*; Springer: New York, 1996.
(30) Berne, B. J.; Pecora, R. *Dynamic Light Scattering*; Wiley: New York, 1976.
(31) Lin, S. C.; Lee, W. I.; Schurr, J. M. *Biopolymers* **1978**, *17*, 1041–1064.
(32) Nojima, Y.; Iguchi, K.; Suzuki, Y.; Sato, A. *Biol. Pharm. Bull.* **2009**, *32*, 523–526.
(33) Miron, T.; Wilchek, M. *Anal. Biochem.* **1982**, *126*, 433–435.
(34) Mours, M.; Winter, H. H. *Macromolecules* **1996**, *29*, 7221–7229.
(35) Winter, H. H.; Mours, M. *Neutron Spin Echo Spectroscopy, Viscoelasticity, Rheology*; Advances in Polymer Science *134*; Springer: New York, 1997; pp 165−234
(36) Cline, G. W.; Hanna, S. B. *J. Org. Chem.* **1988**, *53*, 3583–3586.
(37) Lutolf, M. P.; Hubbell, J. A. *Biomacromolecules* **2003**, *4*, 713–722.
(38) Muthukumar, M. *J. Chem. Phys.* **1997**, *107*, 2619–2635.
(39) Doi, M. *Chem. Phys.* **1975**, *9*, 455–466.